Learning thermal process representations for intraoperative analysis of cortical perfusion during ischemic strokes

$*^{1,2}$, $*^{1}$, $*^{1}$, $*^{2}$, and $*^{3}$

[1] I_1
[2] I_2
[3] I_3

Abstract. Thermal imaging is a non-invasive and marker-free approach for intraoperative measurements of small temperature variations. In this work, we demonstrate the abilities of active dynamic thermal imaging for analysis of tissue perfusion state in case of cerebral ischemia. For this purpose, a NaCl irrigation is applied to the exposed cortex during hemicraniectomy. The caused temperature changes are measured by a thermal imaging system whilst tissue heating is modeled by a double exponential function. Modeled temperature decay constants allow us to characterize tissue perfusion with respect to its dynamic thermal properties. As intraoperative imaging prevents the usage of computational intense parameter optimization schemes we discuss a deep learning framework that approximates these constants given a simple temperature sequence. The framework is compared to common Levenberg-Marquardt based parameter optimization approaches. The proposed deep parameter approximation framework shows good performance compared to numerical optimization with random initialization. We further validated the approximated parameters by an intraoperative case suffering acute cerebral ischemia. The results indicate that even approximated temperature decay constants allow us to quantify cortical perfusion. Latter yield a standardized representation of cortical thermodynamic properties and might guide further research regarding specific intraoperative therapies and characterization of pathologies with atypical cortical perfusion.

Keywords: neurosurgery, intraoperative thermal imaging, deep learning, parameter approximation

1 Introduction

Thermal imaging is a contactless, marker-free, white-light independent and non-invasive method for online measurement of temperature variations up to 30 μK. Current uncooled devices use infrared microbolometer focal plane array detectors measuring a field of view of 16 x 12 cm with an underlying spatial resolution of 250 μm per pixel at a framerate of 50 Hz. The detected infrared radiation

arriving at the microbolometer array is processed and stored as two-dimensional image.
In brain tissue, temperature variations are primarily caused by heat transfers originating from cerebral perfusion. Note, that the local cerebral blood flow correlates with cell metabolism and can be used as marker for tissue state and neural activity. Intraoperative thermal neuroimaging now allows online inference of diagnostic information about perfusion- and neural activity related disorders. [1] demonstrated an approach to distinguish cancerous from healthy tissue based on thermal imaging. [2] evaluated the cortical blood flow by analysing the spatial distribution of a cold bolus applied through a central line with multivariate analysis tools.
In the remaining, the thermal behavior in case of ischemic strokes is analyzed. Latter denote the shortage of substrates of delimited areas of the brain by blockage of vessels (embolism or thrombosis). Severe strokes lead to a swelling of brain tissue, which raises intracranial pressure (ICP) leading to bad or fatal prognosis if not treated appropriately. Hemicraniectomy can be considered as last resort to decrease ICP. We extend the approach of Steiner et al. [2] by combining deep learning and active dynamic thermal imaging during decompressive hemicraniectomy to characterize the perfusion state of cortical tissue. The proposed method integrates seamlessly into typical intraoperative workflows and is not limited to perfused areas in contrast to the Cold Bolus approach of Steiner et al. We also extend prior findings of Gorbach et al. [3] by a sound mathematical model with efficient approximation of tissue thermodynamics yielding standardized parameters of cortical perfusion.

2 Intraoperative Reasoning about Cortical Perfusion

Gorbach et al. [3] proposed irrigating the surface of cortical tissue for some time to propagate heat through several tissue layers. In contrast, we employ available intraoperative tools to prevent the need for additional sterile tools. The surgeon typically has a tool (e.g. syringe) to purge sterile sodium chloride (NaCl) onto tissue. Hereby, it is possible to selectively apply NaCl to a delimited area of the exposed cortex for a specific duration. This irrigation induces a steep drop in temperature followed by a temperature increase caused by heat transfers. In human tissue, this heating correlates with thermodynamic properties of the underlying tissue, thermal conductivity and tissue perfusion state. By modeling this behavior and estimating respective parameters, it is possible to characterize the imaged tissue.

2.1 Modelling Tissue Perfusion

In 1948, Pennes [4] proposed the biologically inspired "Bioheat equation". He proposed the following model to describe internal as well as external influences to the heat distribution in living tissue:

$$c_p \rho \frac{\delta T(x,y,z)}{\delta t} = \kappa \nabla^2 T(x,y,z,t) + q_b + q_m + q_{ex} \tag{1}$$

with the specific heat c_p, material density ρ, temperature distribution $T(x, y, z)$ at time t $T(x, y, z, t)$ and thermal inductivity κ. He further added biological parameters describing the heat power density of q_b blood flow, q_m metabolism and external power density q_{ex}.
Several authors have shown the discretization of Penne's equation (see for example Gutierrez et al. [5]). In our case, we are facing several a priori unknown parameters whose estimation schemes would introduce significant computational complexity and potentially inaccurate estimates. To counter these challenges, we propose to employ Nowakowski's approach to approximate tissue's thermal behavior by a double exponential function [6] at time t

$$T(t, \theta) = T_{equ} + \Delta T_1 exp(-t\gamma_1) + \Delta T_2 exp(-t\gamma_2) \tag{2}$$

$\theta_i = (\Delta T_1, \Delta T_2, \gamma_1, \gamma_2, T_{equ})$ denotes the set of all model parameters with T_{equ} resembling the tissue's equilibrium temperature, ΔT_1 and ΔT_2 being the scaling coefficients of both exponential functions. Decay constants γ_1 and γ_2 (unit s^{-1}) denote the amplitude of the tissue's temperature change rate.
By applying a cold liquid to the exposed cortex, we expect at least two orthogonal components that explain subsequent heating. One component represents the temperature changes of the applied cool fluid. The other component describes the temperature change of the affected underlying tissue. Latter gets dominant after the fluid drained from the surface. Since the cortex can be regarded as convex shape with high curvature, it is reasonable to expect the fluid to drain continuously and fast. We therefore expect γ_2 of the fluid to be larger than γ_1 of the imaged tissue allowing a reliable distinction and therefore estimation of both.

2.2 Levenberg-Marquardt Algorithm

Non-linear least squares is a standard approach for solving eqn. 2. Given n data samples y_i and time points t_i $(1 \leq i \leq n)$ the problem formulation reads

$$\widetilde{\theta} \in \underset{\theta}{argmin} \sum_{i=1}^{n} ||y_i - T(t_i, \theta)||_2^2 := \sum_{i=1}^{n} ||f_i||_2^2$$

Minimizing this equation yields an estimate of thermal perfusion parameters $\widetilde{\theta}$. As the optimization problem is non-linear, iterative optimization schemes are required for minimization. The (damped) Levenberg-Marquardt algorithm (LMA) depicts a fast iterative scheme to estimate $\widetilde{\theta}$ by only relying on the model's Jacobian $J = [J_1^T \dots J_n^T]^T$. Given sample i, row vector $J_i = \delta f_i / \delta \theta$ denotes the gradient of f_i with respect to θ

$$J_i = [-t_i \Delta T_1 exp(t_i\gamma_1) \ -t_i \Delta T_2 exp(t_i\gamma_2) \ -exp(t_i\gamma_1) \ -exp(t_i\gamma_2) \ -1]$$

In each iteration, θ is replaced by $\theta + \nu$ whereas ν is determined by solving

$$(J^T J + \lambda I)\nu = J^T (y - T(\theta))$$

with identity matrix I, some (non-negative) damping factor λ, $y = [y_1 \dots y_n]^T$ and $T(\theta) = [T(t_1, \theta) \dots T(t_n, \theta)]^T$. Depending on the target function and initial values LMA can achieve quadratic convergence [7]. A detailed discussion of LMA can be found elsewhere (see for example [7], [8]).

2.3 Approximating Thermal Process Parameters by Deep Neural Networks

As we have to estimate θ for each pixel of our thermal video sequence even efficient numerical optimization schemes can be time consuming or require a vast amount of computational resources. In order to tackle both challenges, we trained a deep parameter approximation network (DPA) that learns the underlying manifold so that it approximates θ given a length k thermal sequence $(T(t_1), T(t_2), \dots, T(t_k))$. The network is described by some $\eta : \mathbb{R}^k \rightarrow \mathbb{R}^5$. In order to catch non-linear dependencies a regularized (using dropout layers [9]) multi-layer neural network topology is employed. S-shaped rectified linear activation layer [10] further allow to catch non-convex effects. The whole topology of the proposed network is shown in figure 1 and is trained by adaptive moment estimation [11]. As we are approximating the parameter space of an a priori known model, supervised training data is generated by sampling equation 2. This yields a training set $\mathcal{X} = (T_j, \theta_j)$ of m samples with $T_j \in \mathbb{R}^k$, $\theta_j \in \mathbb{R}^5$ and $1 \leq j \leq m$.

3 Results and Discussion

We performed several experiments to evaluate the performance of the proposed irrigation analysis framework. All intraoperative procedures were approved by the Human Ethics Committee. Informed consent was obtained postoperatively in accordance with the approved scheme. In the following, we evaluate the detector's performance in experimental test and training datasets. Afterwards, the approach is used to analyze exemplary intraoperative data. All computations were done on a workstation with dual Intel Xeon E5-2630, 128 GB Ram and Nvidia Geforce GTX Titan Black graphics card.

3.1 Deep Parameter Approximation

Sampling instances (θ^*, T^*) of equation 2 allows us to quantify the performance of the proposed optimization schemes with respect to groundtruth parameter θ^* and synthetic temperature series $T^* = (T_1^*, \dots, T_k)^*$. As baseline method we chose a damped Levenberg-Marquardt optimizing scheme given three parameter initialization strategies. An uninformed guess (RAND) of θ_0 is acquired by sampling $\theta_0^{\mathrm{RAND}} \sim N([0\ 0\ 0\ 0\ 28]^T, \Sigma)$ whereas near-optimal initializations (NO) are realized by sampling $\theta_0^{\mathrm{NO}} \sim N(\theta^*, 0.1\Sigma)$ and should yield best performance. Both strategies employ $\Sigma = I_5$ with I_5 being a 5×5 identity matrix. The last strategy initializes LMA by the output of the deep parameter approximation

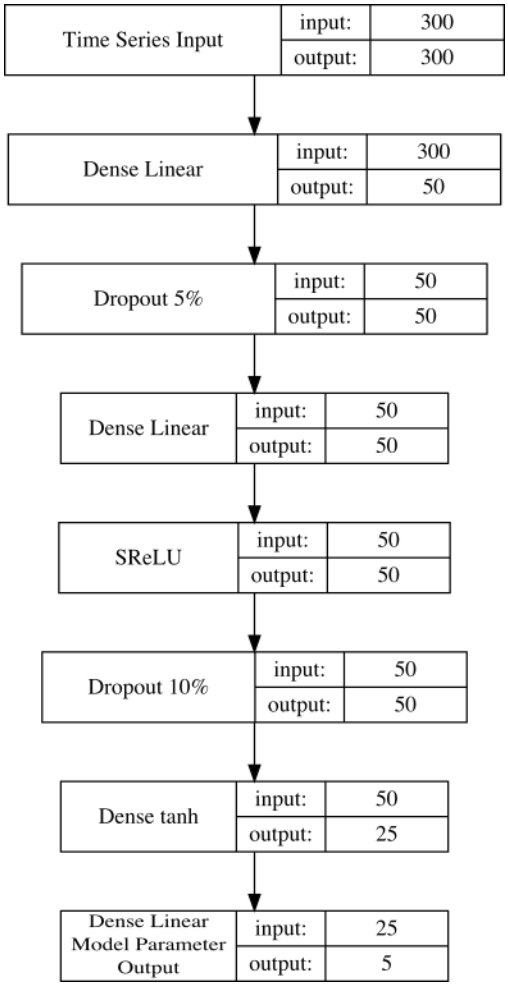

Fig. 1. This figure shows the deep neural network used to approximate thermal perfusion parameters of equation 2.

network given T^* denoted by LMA-DPA: $\theta_0^{\mathrm{DPA}} = \eta(T^*)$. Latter should be close to the optimal solution for what reason we expect better performance than by random initialization.

The accuracy of the parameter estimates $\widetilde{\theta} = [\widetilde{\gamma_1}\ \widetilde{\gamma_2}\ \widetilde{\Delta T_1}\ \widetilde{\Delta T_2}\ \widetilde{T_{equ}}]$ is quantified by two measures $\epsilon = ||\widetilde{\theta} - \theta^*||_2^2$ and $\epsilon_\gamma = ||[\gamma_1^*\ \gamma_2^*]^T - [\widetilde{\gamma_1}\ \widetilde{\gamma_2}]^T||_2^2$. Latter is particularly interesting as the temperature decay constants correlate with cortical perfusion and denote the most important parameters for subsequent analysis. Runtime denotes the time required to optimize a single temperature sequence of length k. The results are shown in table 3.1. The results suggest that DPA approximates the model parameters more accurately than Levenberg-Marquardt

method	iterations	runtime [s]	ϵ	ϵ_γ
DPA	1	0.00001	1.384 ± 0.742	0.098 ± 0.061
LMA-NO	31.64 ± 96.7	0.006	0.63 ± 3.13	0.001 ± 0.006
LMA-DPA	37 ± 81	0.005	$\mathbf{0.026 \pm 0.181}$	$\mathbf{0.0001 \pm 0.0006}$
LMA-RAND	130 ± 147	0.014	2.913 ± 5.325	0.282 ± 0.292

Table 1. This table shows the achieved performance of the proposed deep parameter approximation (DPA) scheme compared to traditional Levenberg-Marquardt based numerical optimization given three different initialization schemes.

optimization with random initialization and significantly reduced overall runtime. When used as initialization for LMA it is interesting to note that the approximated parameters seem to lie close to the actual parameters as LMA-DPA achieves better performance than LMA-NO with less variation.

3.2 Case Study

The examined case suffered an acute ischemic stroke of middle cerebral artery requiring a decompressive hemicraniectomy to decrease intracerebral pressure. Accompanying and without influencing the surgical intervention we performed thermographic measurements of the exposed cortex and recorded intraoperative irrigations of cold NaCl. Latter causes a steep temperature drop and subsequent heating. These irrigations are common in neurosurgery in order to prevent cortical drying. We further segmented the infarct demarcation in postoperative computed tomography (CT) scans and mapped thermal image sequences onto the cortex for easier orientation (figure 2b). Heating parameters were approximated by the discussed DPA approach being applied to the heating sequence caused by the cortical irrigation. Figure 2c visualizes the approximated values of γ_1. Low values of γ_1 indicate reduced perfusion and metabolism which also explains the clear correlation with the infarct demarcation in postoperative CT (see figure 2a).

4 Conclusion

Thermography is an emerging whitelight-independent, non-invasive method to measure the temperature distribution of surfaces. By application of temperature gradients, this method is extended to active dynamic thermography. In medical domain this enables analysis of abnormal tissue and vascular pathologies by dynamic thermal properties.
We employ active dynamic thermography to analyze the perfusion of the exposed human cortex during neurosurgical interventions in case of ischemic strokes. Our approach requires the application of a temperature gradient to the exposed cerebral cortex in order to quantify cortical perfusion. These gradients are induced by applying a cold NaCl irrigation to the exposed cerebral cortex. Subsequent tissue heating is modeled by a double exponential function and its parameter's

are approximated efficiently by a novel deep parameter learning framework. The parameters include thermal decay constants that quantify the rate of tissue heating. We demonstrated that these decay constants correlate with tissue perfusion state and allow to draw conclusions regarding infarct demarcations as imaged by pre/post-operative CT measurements. This enables the surgeon to inspect the progression of cerebral ischemia and allows inferring further diagnostic information. In order to improve clinical significance of our results and enhance the accuracy of our deep parameter approximation network further research on larger cohorts is required. A more advanced parameter approximation network might allow to reliably estimate the parameters of Penne's bioheat equation and therefore infer fine-grain information about tissue composition. We further expect that other pathologies can be characterized by their dynamic thermal behavior as well especially if they correlate with atypical metabolism or perfusion.

Acknowledgment

The authors would also like to thank all other organizations and individuals that supported this research project.

References

1. A. M. Gorbach, J. D. Heiss, L. Kopylev, and E. H. Oldfield, "Intraoperative infrared imaging of brain tumors," *Journal of Neurosurgery*, vol. 101, no. 6, pp. 960–969, 2004.
2. G. Steiner, S. B. Sobottka, E. Koch, G. Schackert, and M. Kirsch, "Intraoperative imaging of cortical cerebral perfusion by time-resolved thermography and multivariate data analysis," *Journal of Biomedical Optics*, vol. 16, no. 1, pp. 016 001–016 006, 2011.
3. A. Gorbach, J. D. Heiss, L. Kopylev, and E. H. Oldfield, "Intraoperative infrared imaging of brain tumors," *Journal of Neurosurgery*, 2004.
4. H. H. Pennes, "Analysis of tissue and arterial blood temperatures in the resting human forearm," *Journal of Applied Physiology*, 1948.
5. G. Gutierrez and M. Giordano, "Study of the bioheat equation using monte carlo simulations for local magnetic hyperthermia," *Proc. ASME 2008 International Mechanical Engineering Congress and Exposition*, 2008.
6. A. Nowakowski, *7. Quantitative active dynamic thermal IR-imaging and thermal tomography in medical diagnostics.* Taylor and Francis, 2013.
7. N. Yamashita and M. Fukushima, *On the Rate of Convergence of the Levenberg-Marquardt Method.* Vienna: Springer Vienna, 2001, pp. 239–249.
8. J. J. Moré, *The Levenberg-Marquardt algorithm: Implementation and theory.* Berlin, Heidelberg: Springer Berlin Heidelberg, 1978, pp. 105–116.
9. N. Srivastava, G. Hinton, A. Krizhevsky, I. Sutskever, and R. Salakhutdinov, "Dropout: A simple way to prevent neural networks from overfitting," *Journal of Machine Learning Research*, vol. 15, pp. 1929–1958, 2014.
10. X. Jin, C. Xu, J. Feng, Y. Wei, J. Xiong, and S. Yan, "Deep learning with s-shaped rectified linear activation units," *CoRR*, vol. abs/1512.07030, 2015.
11. D. P. Kingma and J. Ba, "Adam: A method for stochastic optimization," *CoRR*, vol. abs/1412.6980, 2014.

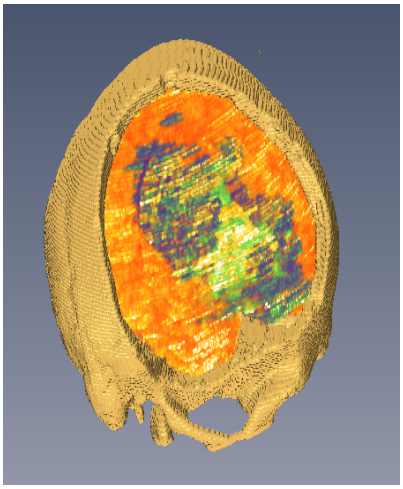

(a)

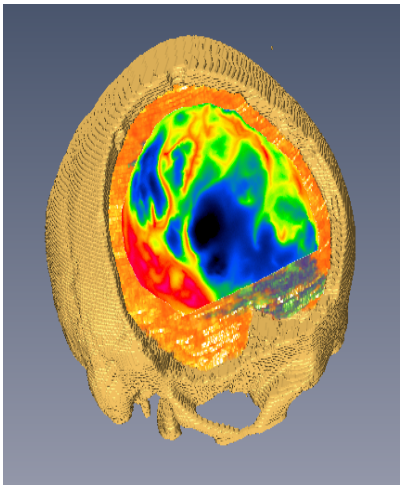

(b)

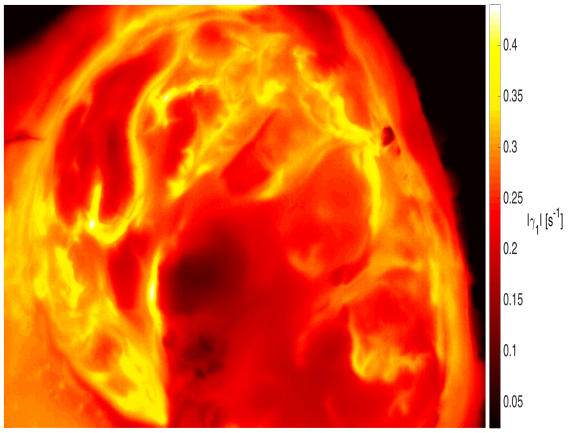

(c)

Fig. 2. Figure **A** visualizes the infarct demarcation as green-blue object in a post-operative CT recording with the convex shape being the trepanation. **B** depicts the temperature distribution at equilibrium temperature after the cortical irrigation. Blue visualizes temperatures at 22 $^{\circ}C$ and red resembles temperatures at 32 $^{\circ}C$. **C** shows the spatial distribution of γ_1. Black represents ischemic / low perfusion state whilst the brighter colors denote stronger perfusion. Note that op towel got hit by cold NaCl irrigation as well causing some heating off the trepanation. The estimated underperfused tissue state correlates with post-operative infarct demarcation. Compared to equilibrium temperature, thermal decay constant γ_1 allows to infer standardized and more detailed information regarding tissue perfusion. The transition between healthy and ischemic tissue (orange to red colors) might be subject for further inspections and therapies.